Journal of Geoscience and Environment Protection, 2022, 10, 82-100
https://www.scirp.org/journal/gep
ISSN Online: 2327-4344
ISSN Print: 2327-4336

A Simplified Concept to Test Erosion or Sedimentation Potential along a Tidal River in the Ganges-Brahmaputra-Meghna Delta

Md. Kabirul Islam[1*], Md. Munsur Rahman[2]

[1]Department of Civil Engineering, Military Institute of Science and Technology (MIST), Dhaka, Bangladesh
[2]Institute of Water and Flood Management (IWFM), Bangladesh University of Engineering and Technology (BUET), Dhaka, Bangladesh
Email: *kabirul_1650@ce.mist.ac.bd, *kabirul189@gmail.com, mmrahman@iwfm.buet.ac.bd, munsurbuet1989@gmail.com

How to cite this paper: Islam, Md. K., & Rahman, Md. M. (2022). A Simplified Concept to Test Erosion or Sedimentation Potential along a Tidal River in the Ganges-Brahmaputra-Meghna Delta. *Journal of Geoscience and Environment Protection, 10,* 82-100.
https://doi.org/10.4236/gep.2022.104006

Received: February 27, 2022
Accepted: April 16, 2022
Published: April 19, 2022

Abstract

The Payra is a tidal river with meandering planform in which around 6.5 km long landmass is formed naturally during the last 40 years that is selected for an establishment by the Government of Bangladesh. However, the site experiences intermittent erosion at several locations and poses threat to the newly developed infrastructures. In the present study, a Rouse type simple model is used to estimate the equilibrium profiles of suspended sediment concentration below which the system is likely to be eroded and regarded as "Sediment Deficit System, SDS" and above which the system is likely to be sedimented and regarded as "Sediment Surplus System, SSS". The model was then tested at the study reach using the measured flow-sediment data complemented by field observation and Landsat images-based planform analysis. The analysis revealed that the residual flow-sediment regime in the study site is representing the "sediment deficit system" that causes continuous threat for erosion throughout the tidal cycles. Therefore, the availability of new landmass should not be the only criterion for the quick selection of a project site, and residual flow-sediment regime needs to consider as an additional parameter for such decision-making process.

Keywords

Suspended Sediment Concentration, Sediment Surplus System, Sediment Deficit System, Residual Flow-Sediment Regime

1. Introduction

Estuarine environment of deltaic river systems is always attractive for human settlements and economic activities because of its valuable ecosystems, natural resources and cost-effective communications, although, there exists a number of inherent threats and challenges experienced by multiple natural hazards such as flooding, erosion, storm surges and salinity coupled with anthropogenic stresses (Ericson et al., 2006; Syvitski et al., 2009). The proximity of the river banks is the most suitable locations for such developments and ensuring the safety against the hazards, specially, the land erosion is one of the important challenges (Akter et al., 2019; Dastagir, 2014; Rahman et al., 2020) for the sustained development activities. Moreover, with the growth of population and economic expansion land reclamation in these environments are widely chosen using a wide range of methods including cross-dams to ensure the emerging required spaces (Rahman et al., 2022). The elevation of the lower region of the Ganges-Brahmaputra-Meghna (GBM) delta, has an average height of 1 - 2 m above mean sea level and large areas of land mass are exposed to natural inundation due to higher tidal amplitude in the tide dominated delta (tidal amplitude ranges from 2 - 7 m from the West to East) that often propagates up to 100 km towards landward direction (Hussain & Tajima, 2017; Nicholls et al., 2018). The estuarine networks in the southwest region of the GBM delta are recognized as an eastern, central, and western estuarine system (henceforth EES, CES, and WES, respectively), connected through several cross channels (Rahman et al., 2022). There exist strong seasonal and spatial variations of water-sediment regime that causes regional and temporal changes of erosion-sedimentation within the estuarine system (Dasgupta et al., 2014; Haque et al., 2016).

Generally, erosion is occurring at locations where transport capacity exceeds the availability of the sediment flux, while sedimentation occurring under the reverse condition when sediment load exceeds its transport capacity. The former case we define here as the condition of "sediment deficit system, SDS" and the latter case, we define as "sediment surplus system, SSS". In semidiurnal tidal environment, the flow-sediment regime changes from flood tide to ebb tide or ebb tide to flood tide that eventually lead towards the changes from SDS to SSS or SSS to SDS, seasonally, fortnightly or even daily, at a fixed location. On the other hand, the development sites generally in need for stable land mass and sustainable navigational routes to facilitate smooth waterway communications. To meet the above requirement, it is important to identify whether the site is dominated by or sediment surplus to facilitating the selection of appropriate sites. Through such processes, the prevailing natural processes can be utilized and the development efforts, repair and maintenance will be at the possible minimum level.

As part of wider development activities (Bangladesh Planning Commission, 2018), the Government of Bangladesh (GoB) has planned to establish a large build up area on a sedimentary deposit along the Payra river, developed in the last 40 years at Lebukhali which is about 60 km upstream from the mouth of Bishkhali/Burishwar estuary (**Figure 1**). The natural formative processes of this land mass (sand bars) through development of bends and cut-offs of the meandering reach are discussed earlier (Islam et al., 2018a) which is further demonstrated

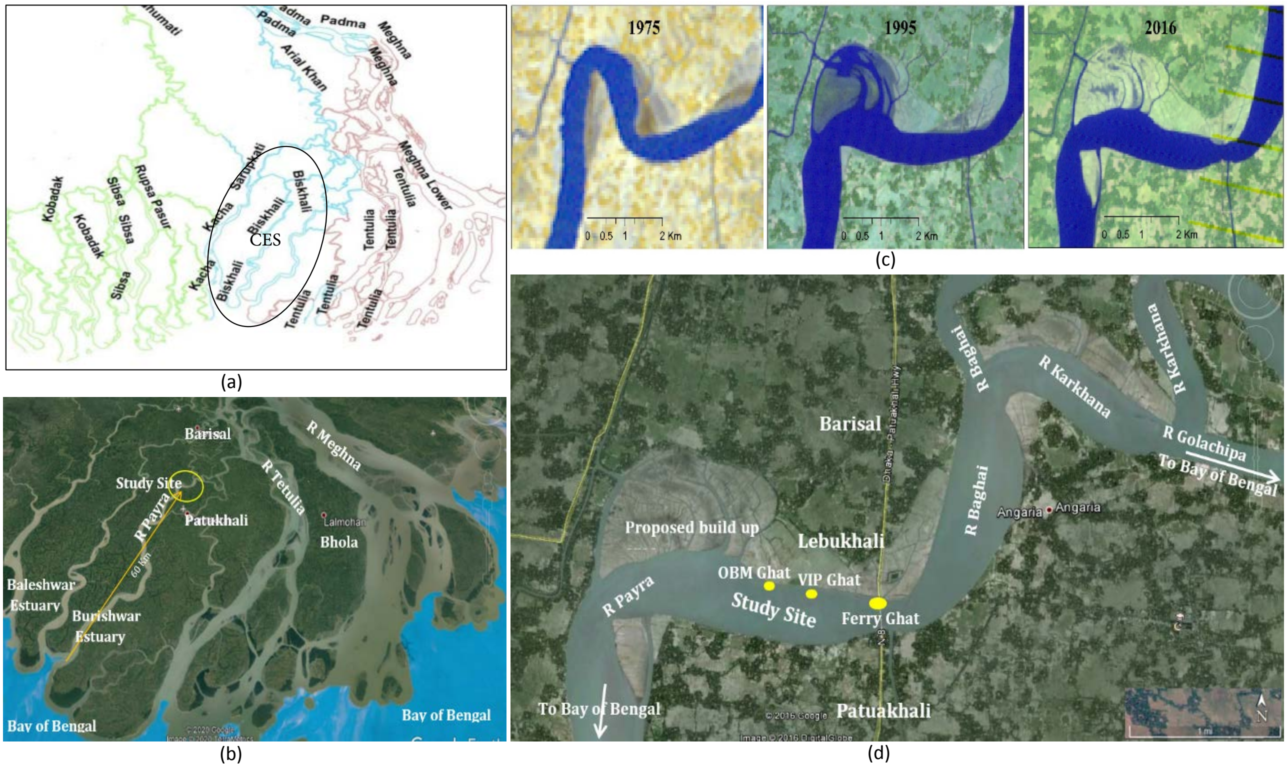

Figure 1. Overall study area, about 60 km upstream from the mouth of Bishkhali/Burishwar estuary. (a) Central estuarine system (CES) of the southern estuarine region of Bangladesh, (b) study site with surrounding districts and river system, (c) evolution of the study area from 1975-2016, and (d) Study site with closer look, 22.274490˚N, 90.173525˚E to 22.301957˚N, 90.214919˚E.

briefly in Figure 1(c). The site is located along the right bank of the Payra river that is tidal in nature. It is located within the CES, is dominated by fresh water, and flows between the districts of Barisal and Patuakhali which are considered as food basket of the country in terms of fisheries and agriculture. The river is linked with the Lower-Meghna through the Tentulia in the north-east, flows to the south and finally falls to the Bay of Bengal through the Bishkhali/Burishwar estuarine mouth. Around 2 km reach of 6.5 km long sedimentary deposit is taken as the study site at the downstream of the existing ferry ghat at which Lebukhai bridge is constructed recently (Figure 1(d)).

The river reaches in this location transports dominantly fresh water and sediment under the complex interactions of fresh water input from the lower Meghna system, tidal exchange, and other fluvial and marine processes. Sediment transport and associated erosion-deposition processes in the study reach is much complicated as it is characterized by the variation of tidal duration, peak velocities and discharges during daily ebb and flood cycles and fortnightly neap-spring cycles as well as slack time during flow reversal. Although the existing four major tidal creeks are kept active during the development work, the study site is still experiencing intermittent bank erosion (Islam et al., 2018b) and the authority needed to manage river erosion in order to continue the planned development activities. Within the above backdrop, the objective of this paper is to identify the reasons of erosion through a confirmative study whether the site is existing within SDS or SSS so that the authority can take appropriate steps to ensure the stability of the developing site.

2. Methodology

The study site does not experience any significant wave action except the seasonal wind induced wave and therefore, only current related suspended sediment transport is considered here. As the sedimentary deposit along the right bank of the study site experiences intermittent erosion as demonstrated by **Figure 2**, with greater intensity during dry season and ebb tide phase, the aim of this paper is to identify the diagnostic reason for the observed erosion through relating the changes of transport capacity at different tidal phases.

2.1. Conceptualization of Sediment Surplus or Sediment Deficit

As the flow induced bed shear velocity (u_*) exceeds a critical value for sediment transport ($u_{*,cr}$), bed particles start moving by sliding, rolling or jumping, usually known as bed load transport. As the vertical component bed shear velocity ($u_{*,cr,sus}$, Equation (1) & (2)) exceeds the particle fall velocity (w_s, Equation (3)), the particle moves in suspension towards the vertical direction (Bagnold, 1966). This movement continues in the direction of flow as if horizontal velocity component is strong enough to carry them away (Guo et al., 2018). The above facts of sediment transport processes are schematically conceptualized in **Figure 3** within the tidal phases, namely during flood and ebb tides.

Critical bed shear velocity ($u_{*,cr,sus}$) for the initiation of suspension can be calculated using the relations of critical Shields parameter for suspension ($\theta_{cr,sus}$) as follows (Soulsby, 1997; van Rijn, 2019):

$$\theta_{cr,sus} = \frac{u_{*,cr,sus}^2}{(s-1)gD} \quad (1)$$

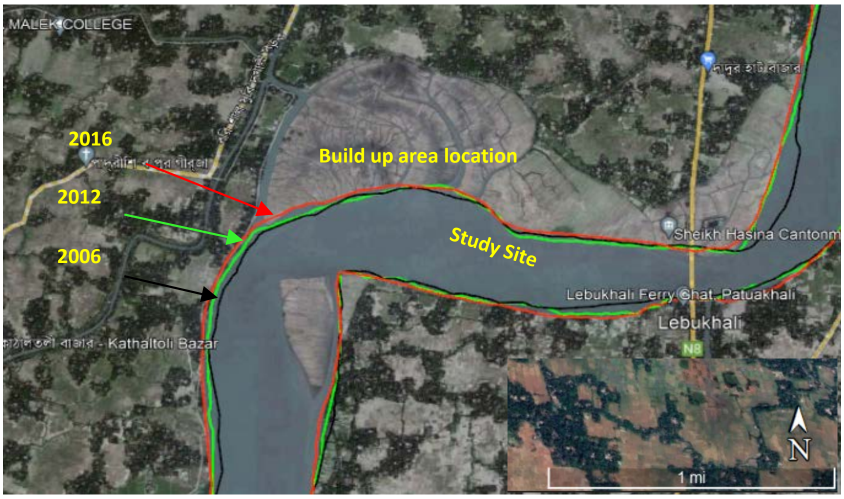

Figure 2. Intermittent erosion-accretion along the bank line of the study site observed during dry season ebb time. Images of 2006, 2012 and 2016. Image: 22.264607˚N, 90.164659˚E to 22.293240˚N, 90.203933˚E.

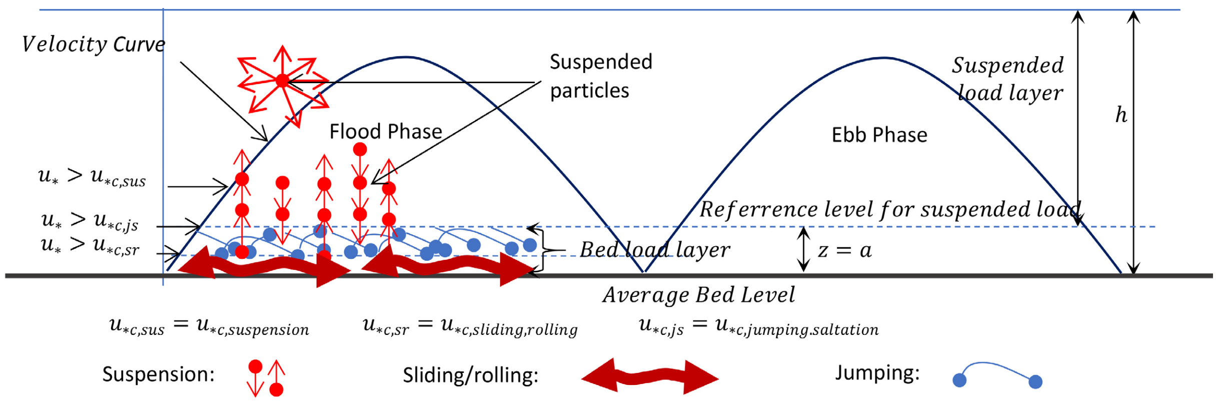

Figure 3. Schematic diagram for sediment transport in a semidiurnal tidal river. Bed load transport takes place in flow direction by sliding or rolling when $u_* > u_{*c,sr}$ and by jumping when $u_* > u_{*c,js}$. Bank and bed material goes for suspension when $u_* > u_{*c,sus}$ or w_s (Hinze, 1975). These suspended particles plus wash load of river and marine flows move horizontally when horizontal component of flow velocity is strong enough to transport them away.

$$\text{and} \quad \theta_{cr,sus} = \frac{0.3}{1+D_*} + 0.1\left[1-\exp\left(-0.05D_*\right)\right] \tag{2}$$

where, the dimensionless grain size parameter $D_* = \left[\frac{(s-1)g}{\upsilon^2}\right]^{1/3} D$.

Particle fall velocity for marine environment can be estimated as follows:

$$w_s = \frac{\nu}{D}\left[\left(10.36^2 + 1.049D_*^3\right)^{\frac{1}{2}} - 10.36\right] \tag{3}$$

where, D is the mean grain size assumed as D_{50}.

However, for the equilibrium transportation of suspended sediment, the volume of deposition caused by gravity must be equal to the volume of upward sediment diffusion, typically conceptualize as $q_{v,downward} = q_{v,upward}$. If the fall velocity w_s of particles of uniform size having the time-averaged suspended sediment concentration (SSC) $C(z)$ at a vertical position z above the bed, the downward volume of flux can be expressed as $q_{v,downward} = w_s C(z)$, while the upward volume flux of particles can be expressed as $q_{v,upward} = \varepsilon_s \frac{\mathrm{d}C(z)}{\mathrm{d}z}$ (**Figure 4**) where ε_s is the vertical diffusion coefficient (Keetels, Goeree, & van Rhee, 2018).

Equating the two fluxes gives an expression for the vertical distribution of SSC in equilibrium over the depth (Nie et al., 2017; van Rijn, 1993, 2012) as

$$w_s C(z) = -\varepsilon_s \frac{\mathrm{d}C(z)}{\mathrm{d}z}$$

$$\text{Or,} \quad w_s C(z) + \varepsilon_s \frac{\mathrm{d}C(z)}{\mathrm{d}z} = 0 \tag{4}$$

In Equation (4), the diffusion coefficient ε_s is assumed proportional to the kinematic eddy viscosity, ν_t as, $\varepsilon_s = \beta \nu_t$ with, $\nu_t = \kappa u_* \frac{z}{h}\left(1-\frac{z}{h}\right)$ (Tsujimoto, 2010) and the Equation can be solved as (Rouse, 1937):

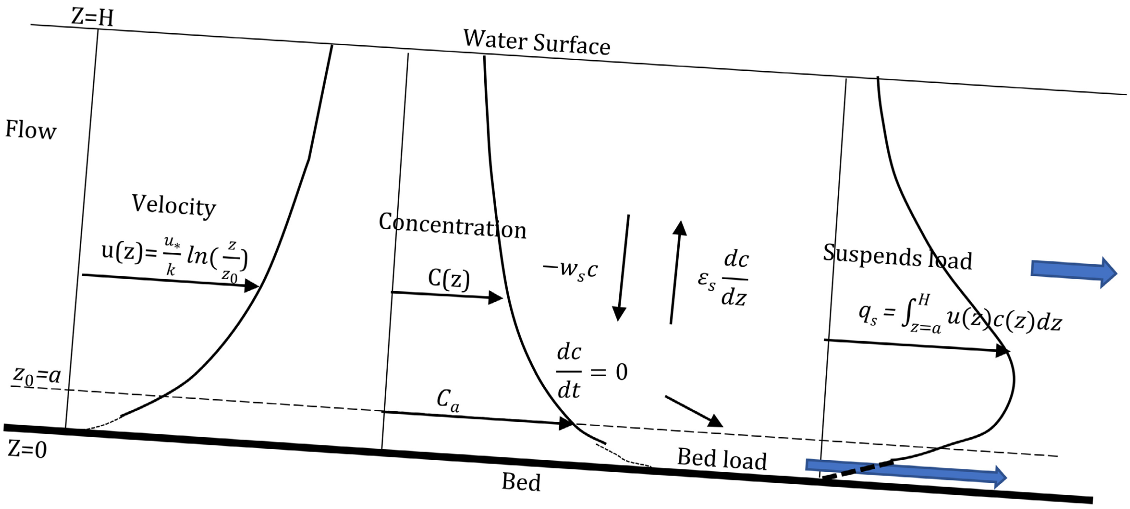

Figure 4. Suspended sediment transport. Volume of suspension $q_{v,upward}$ and deposition $q_{v,downward}$ at bottom boundary layer ($z_0 = a$) for suspension will be equal i.e. $w_s C(z) = \varepsilon_s \frac{\mathrm{d}C(z)}{\mathrm{d}z}$.

$$\frac{C(z)}{C(a)} = \left[\left(\frac{h-z}{z}\right)\left(\frac{a}{h-a}\right)\right]^N \quad \text{with} \quad N = \frac{w_s}{\beta \kappa u_*} \tag{5}$$

where, $C(a)$ = reference concentration at reference level a above river bed, h = flow depth, z = height above the bed level. Here, N is known as suspension number or Rouse number by which the relative distribution of the suspended sediment transport is determined. κ = Karman's constant = 0.4, and β = dimensionless proportionality coefficient related to diffusion of sediment particles.

Equation (5) is widely known as Rouse equation which is used to estimate equilibrium profiles of vertical sediment concentration in tidal and non-tidal rivers (Van Rijn, 1984; Wu et al., 2017). Quantitatively, if the actual sediment concentration exceeds the value of the estimated equilibrium concentration, the hydraulic condition is recognized here as sediment surplus, while the condition is considered as sediment deficit if the actual sediment concentration is less than the equilibrium value. However, in Equation (6), the vertical concentration profile depends significantly on the selection of appropriate reference height a and reference sediment concentration $C(a)$. It is found in several previous researches (Garde & Ranga Raju, 1977; Parker, 1990; Singh et al., 2004) that value of a can be estimated as a function of either flow depth or particle diameter. For plain bed condition, the selection of a based on particle diameter might be applicable but for rough bed, the estimation of a can be done related to flow depth or bed roughness height. The real life field condition is usually representing rough bed which is also valid in the study site. As the measurement of roughness height is relatively difficult in field condition, the choice of appropriate value of a would be evaluated as a function of flow depth (0.01h to 0.05h) as prescribed in previous researches (Engelund & Fredsoe, 1976; Garcia & Parker, 1991; Shibayama & Winyu, 1993; Van Rijn, 1984; Zyserman & Fredsoe, 1994). To estimate another important parameter $C(a)$ at reference level, either the numerical expression (Equation (6)) prescribed by van Rijn (1984, 2007) can be used or the value can be measured in the field.

$$C(a) = 0.015 \frac{d_{50} T^{1.5}}{a d_*^{0.3}} \tag{6}$$

where, T = transport stage parameter $= \frac{u_*^2 - u_{*,cr}^2}{u_{*,cr}^2}$.

2.2. Measurement of Flow and Sediment Parameters

To evaluate the parameters in Equations (2)-(6), required arrangements to collect flow and sediment data were established in the field and data collection continued over the period of 5 years from May 2016 to January 2020. Different sensors coupled with total station/RTK GPS were deployed to measure the spatial and temporal changes of flow, depth, sediment concentration and related parameters (Islam et al., 2021). ADCP is used to measure the velocity and discharge data across the river at different sections of the study site. Vertical velocity profiles are then retrieved from this ADCP records which are used for subsequent analyses. Peak ebb velocities are found varying from 0.59 to 0.79 m/s and peak flood velocities varying from 0.52 to 0.70 m/s in the upstream (VIP Ghat) to downstream location (OBM Ghat). Eco-sounder is used for river bathymetry, and Total Station/RTK GPS is used for horizontal location, digital elevation, and water level data. OBS-3A sensor was mounted on a steel frame and placed 2 m above the bed level at both locations to measure the turbidity from 7 am to 6 pm, in a specified day. The suspended solid concentration at the same locations were also measured. The measured suspended solid concentration and OBS turbidity reading were then calibrated. The calibrated equation was then used to calculate the SSC. The bathymetry and water level data were measured covering the entire study reach, while detailed of sediment concentration and flow velocities were measured at two locations, the OMB Ghat and VIP Ghat (**Figure 1**) at different vertical points within different tidal phases. Grain size analysis was done to estimate the sediment characteristics as well as transport parameters of the river reach.

3. Results and Discussions

3.1. Estimated Parameters

Peak flow velocities for flood and ebb tides, grain size, fluid properties were used to calculate the various hydrodynamic parameters. Summary of the estimated parameters in Equations (1)-(6) are shown in **Table 1**, whereas, details of measured data and estimation of required parameters are discussed in the supplementary.

Here, the reference concentration $C(a)$ is taken at reference height, a = 0.15 to 0.165 m (which is the average of 0.01h to 0.05h), while h varies between 5 to 6 m.

Table 1. Summary of different hydrodynamic parameters.

Parameters	VIP Ghat	OBM Ghat	Equations
Current related shear velocity, u_* (m/s)	FT = 0.054 FE = 0.063	FT = 0.074 FE = 0.085	$u(z)=\frac{u_*}{k}\ln\left(\frac{z}{z_0}\right)$
Current related shear stress τ_b (Nm^{-2})	FT = 2.94 FE = 4.12	FT = 5.57 FE = 7.41	$\tau_b=\rho_w u_*^2$
Dimensionless grain size, D_*	2.38 ≈ 2.4	2.39 ≈ 2.4	$D_*=\left[\frac{(s-1)g}{\upsilon^2}\right]^{1/3}D_{50}$
Critical shear velocity $u_{*,cr,suspension}$ (m/s)	0.0128	0.0128	$\theta_{cr,s}=\frac{u_{*,cr,sus}^2}{(s-1)gD}=\frac{w_s^2}{(s-1)gD}=\frac{0.3}{1+D_*}+0.1\left[1-e^{-0.05D_*}\right]$
Settling velocity, w_s (m/s)	0.0073	0.0073	$w_s=\frac{\nu}{D}\left[\left(10.36^2+1.049D_*^3\right)^{\frac{1}{2}}-10.36\right]$
Rouse number, N	FT = 0.34 FE = 0.29	FT = 0.25 FE = 0.22	$N=\frac{w_s}{\beta\kappa u_*}$
Reference concentration, C_a (mg/l) at a = 0.155 m	FT 690.0 FE 406.7	FT 560.0 FE 156.2	Field data analyzed in laboratory
Transport stage parameter, T	FT = 16.8 FE = 23.0	FT = 32.4 FE = 43.0	$\frac{\tau_b-\tau_{cr}}{\tau_{cr}}$ or $\frac{u_*^2-u_{*,cr}^2}{u_{*,cr}^2}$

The Rouse number N, during the peak ebb and peak flood flow varies 0.25 to 0.22 at OBM Ghat and the above values are relatively higher in the VIP Ghat (0.29 to 0.34). While the corresponding transport stage parameter, T, during the peak flood and peak ebb flow varies 32 to 43 at OBM Ghat and the above values are relatively lower in the VIP Ghat (16 to 23). It is important to note that the higher value of N indicates the lower level of equilibrium sediment concentration. As N values in VIP Ghat are higher than OBM Ghat, the transport capacity in the VIP Ghat is lower as compared with the OBM Ghat. Moreover, the transport stage during the ebb tide is higher as compared with flood tide in both locations which indicates the sediment transport is higher during the ebb tide and residual transport occurred along the ebb direction.

3.2. Sensitivity of Rouse Number on Vertical Profiles of Sediment Concentration

Using $C(a)$ is equal to 690 mg/l and a is equal to 0.15 m, and the sensitivity of N on the vertical concentration of sediment profiles are show in Figure 5.

It is seen that the larger the value of N, the more rapidly the suspended-sediment concentration decreases with height above the reference level, a. The value of N is a function of flow induced shear velocity and particle fall velocity. The particle fall velocity is primarily governed by the particle characteristic and fluid property which generally remain constant for a particular river segment, whereas, the value of flow velocity can be modified often due to anthropogenic interventions. Thereby, the value of N can be increased or decreased to meet the specific requirements of the site. If a site needs sedimentation for land reclamation, the

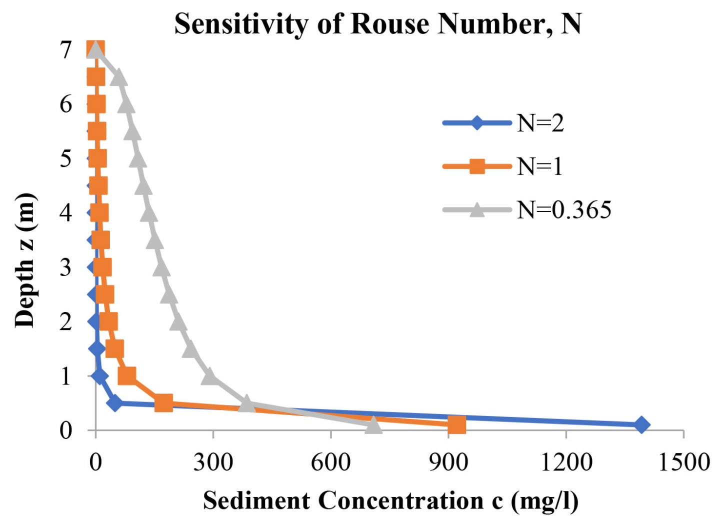

Figure 5. Vertical distribution of SSC for different *N* values. The smaller the *N* value, the larger the sediment concentration.

required value for *N* can be adjusted through suitable interventions. Reverse situation can be also ensured where lowering of riverbed is essential, for example in navigational routes or landing ports.

3.3. Testing for Sediment Deficit System or Sediment Surplus System

Using the required parameters calculated from measured data, sediment concentration profiles are plotted and compared with the equilibrium profiles which are estimated using Equation (5) for both the upstream (VIP Ghat) and downstream (OBM Ghat) locations. The equilibrium profiles are then compared with the measured concentration of those locations during full tide and full ebb. The selection of reference level *a* and corresponding reference concentration $C(a)$ are important to have an accurate distribution profile. Criteria for selecting reference height are already discussed. Since measured sediment concentrations of the study site are available, the estimated reference sediment concentration obtained using Equation (6) is not used here. SSC were measured for four different time periods of a tidal cycle; half tide, full tide, half ebb and full ebb (shown in supplementary). Considering the sensitivity of reference concentration on the distribution profile, these profiles are plotted considering the specific reference concentration of different tidal periods as shown in Figure 6.

The profiles show that the differences between equilibrium concentration and measured concentration are different in full tide and full ebb situations at both upstream and downstream locations. The difference between measured concentration and equilibrium concentration is less in the upstream location but more in the downstream location. This implies downstream location exhibits higher SD and hence more liable to erosion than upstream location. Again, in the upstream or downstream locations, concentration profiles are different during tide and ebb phases. In the upstream, measured concentration nearly merges with

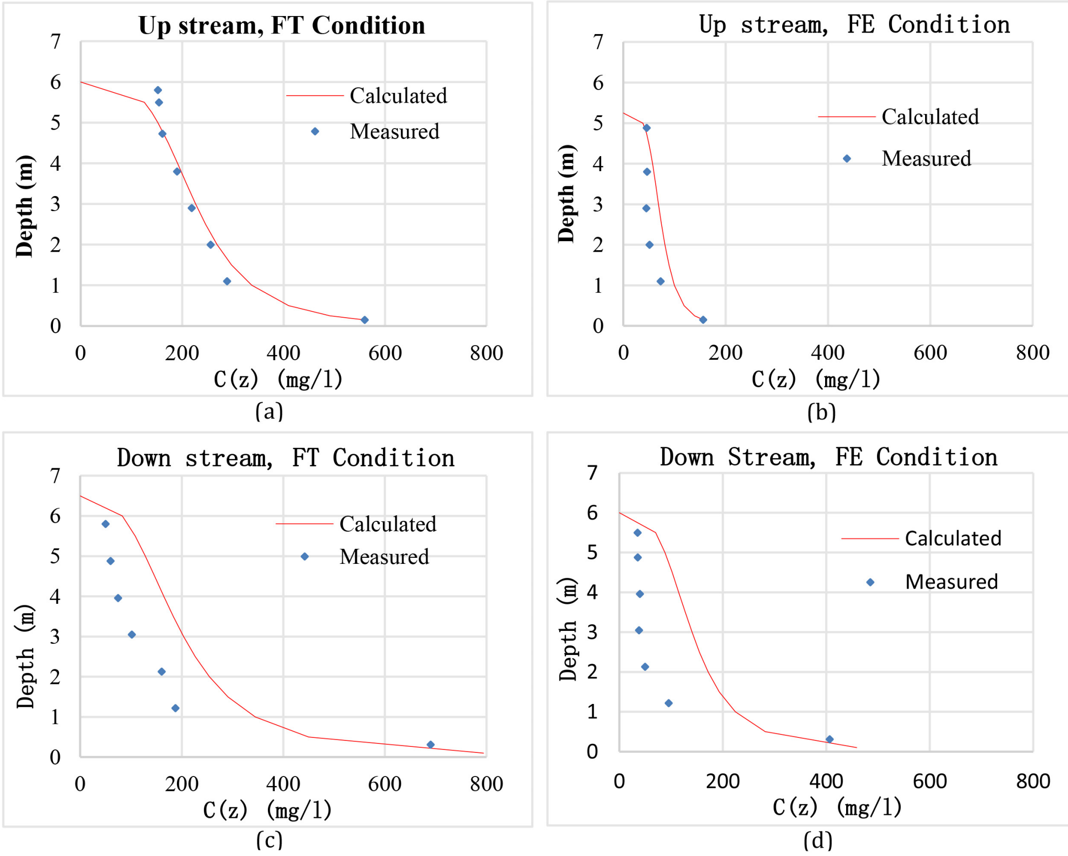

Figure 6. Depth averaged SSC profiles: measured vs. equilibrium. (a) Upstream VIP Ghat location during full tide (FT), (b) upstream VIP Ghat locations full ebb (FE), (c) downstream OBM Ghat location during full tide and (b) downstream OBM Ghat locations during full ebb. The difference between measured concentration and equilibrium concentration is less in the upstream location (a & b) but more in the downstream location (c & d). Again, within upstream or downstream locations, difference between measured concentration and equilibrium concentration is more during FE than FT.

the equilibrium concentration during full tide but lags behind the equilibrium concentration during full ebb. This implies the site is nearly in the equilibrium condition during full tide but remain in SD condition during full ebb and hence more prone to erosion during ebb. In the downstream, measured concentration is found significantly less than the equilibrium concentration during both full tide and full ebb but the difference is more during ebb phase than tide phase. This means the downstream location remains in SD condition and is liable for erosion throughout the tidal cycle. Moreover, the profiles show that SD is more during ebb than during flood which implies that the ebb flow has more sediment transport capacity than the tidal flow. Therefore, intensity of erosion is more during ebb phase than during tide phase. To attain the equilibrium condition, additional sediment supply is required which would come from bank or bed erosion. Therefore, the analysis reveals that the overall status of the study site is sediment deficit condition and thus the site is subject to riverbank or bed erosion. This phenomenon matches quite well with the field condition as it is noticed during field observation and data collection. The field scenario reveals that bank line of 7 - 10 m width particularly in the downstream location had been washed away in last 4 - 5 years period with greater intensity during ebb phase. The above field observations support the hypothesis that system is SD and erosion may continue in the future. Again the time series plot of bank lines in Figure 7 (reproduced from google earth), confirm that during the period of 2006-2012, the total land loss was around 0.56 km^2, while during the period of 2012-2016, the lost land was around 0.33 km^2 which translate a consistent erosion rate of around 0.09 km^2/year. While the rate of accretion translates within the above period with a much lower value which is around 0.01 km^2/year (around 1/10th). The above quantitative analysis of images, validates that the site is erosion dominating that need continuous attention to protect land.

3.4. Implications to Sediment Management

Sediment management is one of the big challenges and less explored issue in the GBM delta which is very important to materialize the inherent opportunities with efficient use of incoming sediment as resource in these environments. The practiced methods are focusing either to accelerate the siltation or de-siltation based on the requirements. For accelerating siltation, cross-dams are typically applied in the coastal zone to trap the sediment for land reclamation which has some inherent consequences to the adjacent areas to initiate or accelerate fresh erosion (Rahman et al., 2022). Tidal river management (TRM) are usually implemented to elevate low lying land inside polders with additional benefit of increased conveyance capacity of the adjacent rivers (Talchabhadel et al., 2020). Bandal-like structures are adopted to increase the conveyance capacity of the navigational routes and ports and enhance near bank sedimentation (Rahman et al.,

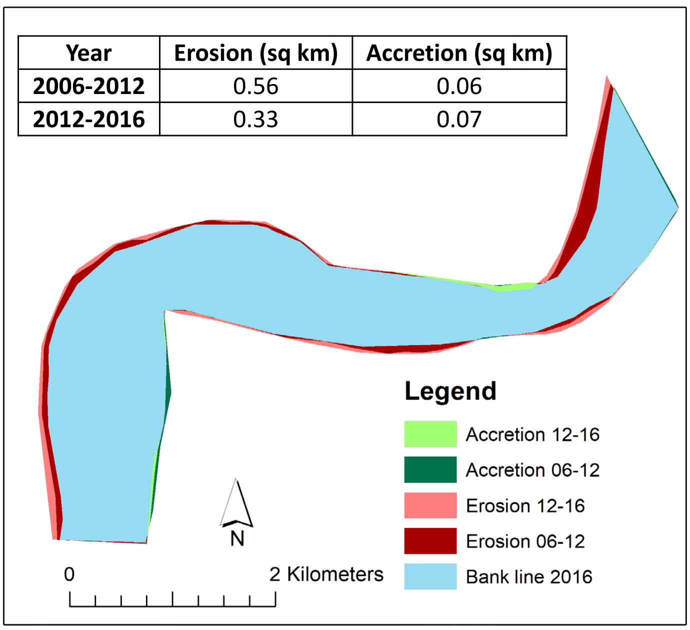

Year	Erosion (sq km)	Accretion (sq km)
2006-2012	0.56	0.06
2012-2016	0.33	0.07

Figure 7. Image analysis for the validation of SDS. The site was in SDS throughout the tidal cycle. That is why, the quantity of erosion in found significant.

2020; Kibriya, 2020). Dredging, on the other hand, is adopted for the maintenance of navigational depths in rivers and recently been applied to solve waterlogging problems within polders (WARPO & BUET, 2020). As the working principles of the methods are different and are applied in isolation depending on the objectives, the interactions within each of the methods are also relatively unknown (Rahman et al., 2022). Therefore, the identification of SDS and SSS will enable to adopt site specific appropriate measures and/or its combinations for sediment management. Through the application of remote sensing and GIS, the real time distribution of sediment concentration is possible to evaluate that can be further utilized to identify whether site is sediment surplus or sediment deficit. Such an insight on the prevailing morpho-dynamic behaviour will be very useful in devising an appropriate solution for river channel stabilization and maintenance of navigational channel and ports.

There exists plenty of examples where river management projects are unsuccessful in Bangladesh, specially, in the estuarine environment because of the inappropriate sediment management options. The improved understanding of whether it is sediment deficit or sediment surplus, may help to avoid the further negative consequences. Further, early identification would provide warning for subsequent erosion or accretion that can enable to take timely countermeasures and thereby could minimize the losses and save the important installations.

4. Conclusion

The selection of appropriate sites in terms of physical stability in the tidal environment is very important to reduce the challenges related to required repair and maintenance against the changes of river channels. The undesirable erosion-scouring-siltation often leads to the unsustainability of the project site leading to the complete failure. Therefore, methodology adopted in the present study to evaluate sediment deficit or sediment surplus can identify the river reach whether it will be an eroding or siltation dominated site which in turn will create the ground for technical justification in the selection processes of a development project site. The study site is selected for the establishment of major infrastructures with the understanding that the sedimentary deposit will remain stable. However, the findings from this study reveal that the site, in general, is representing the SDS with residual sediment transport towards the ebb direction that will experience continuous riverbank erosion. More specifically, the downstream reach with higher depth exhibits more transport capacity than upstream and the ebb phase experiences more sediment deficit than tide phase. Consequently, the concerned river reach needs appropriate bank protection measures to ensure the physical stability of the project.

Further field validation is required to test this method in sediment deficit region in the future through which the above method can be replicable to other sites to understand whether a certain reach of a river system exists within the sediment deficit or sediment surplus and can be an important technique for the selection of stable project site. Moreover, it can be regarded as the precursor of likely erosion or sedimentation and appropriate measures can be adapted accordingly. Real time flow-sediment data would complement in developing a sound sediment management for implementable and environmentally adaptable development plan which needs to be explored in the future.

Conflicts of Interest

The authors declare no conflicts of interest regarding the publication of this paper.

References

Akter, R., Asik, T. Z., Sakib, M., Akter, M., Sakib, M. N., Al Azad, A. S. M. A. et al. (2019). The Dominant Climate Change Event for Salinity Intrusion in the GBM Delta. *Climate, 7,* Article No. 69. https://doi.org/10.3390/cli7050069

Bagnold, R. A. (1966). *An Approach to the Sediment Transport Problem from General Physics*. US Government Printing Office. https://doi.org/10.3133/pp422I

Bangladesh Planning Commission (2018). Bangladesh Delta Plan 2100 (Abridged Version). General Economics Division (GED), Ministry of Planning, Government of the People's Republic of Bangladesh. www.plancomm.gov.bd

Dasgupta, S., Huq, M., Khan, Z. H., Ahmed, M. M. Z., Mukherjee, N., Khan, M. F., & Pandey, K. (2014). Cyclones in a Changing Climate: The Case of Bangladesh. *Climate and Development, 6,* 96-110. https://doi.org/10.1080/17565529.2013.868335

Dastagir, M. R. (2014). Modeling Recent Climate Change Induced Extreme Events in Bangladesh: A Review. *Weather and Climate Extremes, 7,* 49-60. https://doi.org/10.1016/j.wace.2014.10.003

Engelund, F., & Fredsoe, J. (1976). A Sediment Transport Model for Straight Alluvial Channels. *Hydrology Research, 7,* 293-306. https://doi.org/10.2166/nh.1976.0019

Ericson, J. P., Vörösmarty, C. J., Dingman, S. L., Ward, L. G., & Meybeck, M. (2006). Effective Sea-Level Rise and Deltas: Causes of Change and Human Dimension Implications. *Global and Planetary Change, 50,* 63-82. https://doi.org/10.1016/j.gloplacha.2005.07.004

Folk, R. L. (1974). *Petrology of Sedimentary Rocks* (p. 182). Hemphill.

Garcia, M., & Parker, G. (1991). Entrainment of Bed Sediment into Suspension. *Journal of Hydraulic Engineering, 117,* 414-435. https://doi.org/10.1061/(ASCE)0733-9429(1991)117:4(414)

Garde, R. J., & Ranga Raju, K. G. (1977). *Mechanics of Sediment Transportation and Alluvial Stream Problems* (pp. 157-183). Wiley Eastern Limited.

Guo, L., Brand, M., Sanders, B. F., Foufoula-Georgiou, E., & Stein, E. D. (2018). Tidal Asymmetry and Residual Sediment Transport in a Short Tidal Basin under Sea Level Rise. *Advances in Water Resources, 121,* 1-8. https://doi.org/10.1016/j.advwatres.2018.07.012

Haque, A., Sumaiya, & Rahman, M. (2016). Flow Distribution and Sediment Transport Mechanism in the Estuarine Systems of Ganges-Brahmaputra-Meghna Delta. *International Journal of Environmental Science and Development, 7,* 22-30. https://doi.org/10.7763/IJESD.2016.V7.735

Hinze, I. O. (1975). *Turbulence* (2nd ed., pp. 640-645). McGraw-Hill Book Co., Inc.

Hussain, M. A., & Tajima, Y. (2017). Numerical Investigation of Surge-Tide Interactions in the Bay of Bengal along the Bangladesh Coast. *Natural Hazards, 86,* 669-694. https://doi.org/10.1007/s11069-016-2711-4

Islam, M. K., Al Kibriya, N., & Dustegir, M. M. (2018b). Impact Analysis of Sand Dredging from Alluvial Tidal River. *E3S Web of Conferences, 40,* Article No. 03036. https://doi.org/10.1051/e3sconf/20184003036

Islam, M. K., Al Kibriya, N., & Rahman, M. M. (2021). Assessment of Morphodynamic Baseline of a Tidal River. *Book of Abstract, 8th International Conference on Water and Flood Management* (p. 184). Institute of Water and Flood Management (IWFM), BUET, Dhaka, Bangladesh. https://iwfm.buet.ac.bd/site/iwfm/icwfm2021

Islam, M. K., Dushtagir, M., Rahman, M. M., & Rahman, M. (2018a). Changes in Planform and Meander Bends of Rivers in Southern Estuarine Region of Bangladesh and Its Implications on Development Project. *Global Science and Technology Journal, 6*, 17-26.

Keetels, G. H., Goeree, J. C., & van Rhee, C. (2018, January 2). Advection-Diffusion Sediment Models in a Two-Phase Flow Perspective. *Journal of Hydraulic Research, 56,* 136-140. https://doi.org/10.1080/00221686.2017.1289262

Kibriya, N. A. (2020). *Performance Evaluation of Bandal-Like Structures for Tidal River Flow and Sediment Management*. Unpublished Msc Thesis, Intitute of Water and Flood Management, Bangladesh University of Engineering and Technology.

Nicholls, R. J., Hutton, C. W., Adger, W. N., Hanson, S. E., Rahman, M. M., & Salehin, M. (2018). Integrative Analysis for the Ganges-Brahmaputra-Meghna Delta, Bangladesh. In R. Nicholls, C. Hutton, W. Adger, S. Hanson, M. Rahman, & M. Salehin (Eds.), *Ecosystem Services for Well-Being in Deltas* (pp. 71-90). Palgrave Macmillan. https://doi.org/10.1007/978-3-319-71093-8_4

Nie, S., Sun, H. G., Zhang, Y., Chen, D., Chen, W., Chen, L., & Schaefer, S. (2017). Vertical Distribution of Suspended Sediment under Steady Flow: Existing Theories and Fractional Derivative Model. *Discrete Dynamics in Nature and Society, 2017,* Article ID: 5481531. https://doi.org/10.1155/2017/5481531

Parker, G. (1990). Surface Based Bed Load Transport Relationships. *Journal of Hydraulic Research, 28*, 417-436. https://doi.org/10.1080/00221689009499058

Rahman, M. A., Rahman, M. M., Shampa, Haque, A., Dustegir, M. M., Nishat, N. J. et al. (2020). Performance Evaluation of Bandal-Like Structures for Sediment Management in Braided Jamuna River. *Proceedings of the 22nd Congress of the International Association for Hydro-Environment Engineering and Research-Asia Pacific Division (IAHR-APD Congress 2020): Creating Resilience to Water-Related Challenges* (pp. 1-6). IAHR. https://www.proceedings.com/content/058/058441webtoc.pdf

Rahman, M. M., Haque, A., Nicholls, R. J., Darby, S. E., Urmi, M. U., Dustegir, M. M. et al. (2022). Sustainability of the Coastal Zone of the Ganges-Brahmaputra-Meghna Delta under Climatic and Anthropogenic Stresses. *Science of the Total Environment, 829,* Article ID: 154547. https://doi.org/10.1016/j.scitotenv.2022.154547

Rouse, H. (1937). *Nomogram for the Settling Velocity of Spheres* (pp. 57-64). National Research Council.

Shibayama, T., & Winyu, R. (1993). Vertical Distribution of Suspended Sediment Concentration in and Outside Surf Zone. *Coastal Engineering in Japan, 36,* 49-65. https://doi.org/10.1080/05785634.1993.11924573

Singh, A. K., Kothyari, U. C., & Ranga Raju, K. G. (2004). Rapidly Varying Transient Flows in Alluvial Rivers. *Journal of Hydraulic Research, 42,* 473-486. https://doi.org/10.1080/00221686.2004.9641217

Soulsby, R. (1997). Dynamics of Marine Sands. 1 Heron Quay, London E14 4JD: Thomas

Telford, UK.

Syvitski, J. P. M., Kettner, A. J., Overeem, I., Hutton, E. W. H., Hannon, M. T., Brakenridge, G. R. et al. (2009). Sinking Deltas Due to Human Activities. *Nature Geoscience, 2,* 681-686. https://doi.org/10.1038/ngeo629

Talchabhadel, R., Nakagawa, H., & Kawaike, K. (2020). Selection of Appropriate Shifting of Tidal River Management. In A. Haque, & A. I. A. Chowdhury (Eds.), *Water, Flood Management and Water Security under a Changing Climate* (pp. 283-299). Springer. https://doi.org/10.1007/978-3-030-47786-8_20

Tsujimoto, T. (2010). Diffusion Coefficient of Suspended Sediment and Kinematic Eddy Viscosity of Flow Containing Suspended Load. *River Flow 2010, No. 3,* 801-806. http://scholar.google.com/scholar

Van Ledden, M., Van Kesteren, W. G. M., & Winterwerp, J. C. (2004). A Conceptual Framework for the Erosion Behaviour of Sand-Mud Mixtures. *Continental Shelf Research, 24,* 1-11. https://doi.org/10.1016/j.csr.2003.09.002

van Rijn, L. (2012). *Principles of Sediment Transport in Rivers, Estuaries and Coastal Seas* (pp. 1-17). Aqua Publications.

Van Rijn, L. C. (1984). Sediment Transport, Part II: Suspended Load Transport. *Journal of Hydraulic Engineering, 110,* 1613-1641. https://doi.org/10.1061/(ASCE)0733-9429(1984)110:11(1613)

van Rijn, L. C. (1993). *Simple General Formulae for Sand Transport in Rivers, Estuaries and Coastal Waters*. http://www.leovanrijn-sediment.com

van Rijn, L. C. (2007). Unified View of Sediment Transport by Currents and Waves. II: Suspended Transport. *Journal of Hydraulic Engineering, 133*, 668-689.

van Rijn, L. C. (2019). Erodibility of Mud-Sand Bed Mixtures. *Journal of Hydraulic Engineering, 146*, Article ID: 04019050. https://doi.org/10.1061/(ASCE)HY.1943-7900.0001677

Water Resources Planning Organisation (WARPO), & Bangladesh University of Engineering and Technology (BUET) (2020, September). *Research on Sediment Distribution and Management in South-West Region of Bangladesh*. Interim Report, Institute of Water and Flood Management (IWFM), Bangladesh University of Engineering and Technology.

Wu, G., Zhua, L., & Li, F. (2017). Mean Velocity and Suspended Sediment Concentration Profile Model of Turbulent Shear Flow with Probability Density Function. *Earth Sciences Research Journal, 21,* 129-134. https://doi.org/10.15446/esrj.v21n3.65172

Zyserman, J. A., & Fredsoe, J. (1994). Data Analysis of Bed Concentration of Suspended Sediment. *Journal of Hydraulic Engineering, 120,* 1021-1042. https://doi.org/10.1061/(ASCE)0733-9429(1994)120:9(1021) http://www.ascelib

Supplementary: Measured Data and Estimation of Required Parameters

Velocity profile

Velocity data are measured using ADCP across the river at different sections. Vertical velocity profiles of two locations about 20 m away from the bank line were retrieved from ADCP records for both ebb and flood peaks. The vertical velocity profiles are shown in Figure S.1.

Suspended sediment data

Sediment sample were collected from two locations (VIP Ghat and OBM Ghat, 0.6 km away from each other) using OBS and manually using improvised sample collector. The results are shown in Table S.1 and Table S.2 below respectively for two locations 0.6 km away from each other. Samples were collected with respect to local measurement unit feet and then converted to metric unit.

Bed soil data

River bed sample were collected from both VIP Ghat and OBM Ghat locations of the study site and grain size distributions are done. The results are shown in Table S.3 and Table S.4.

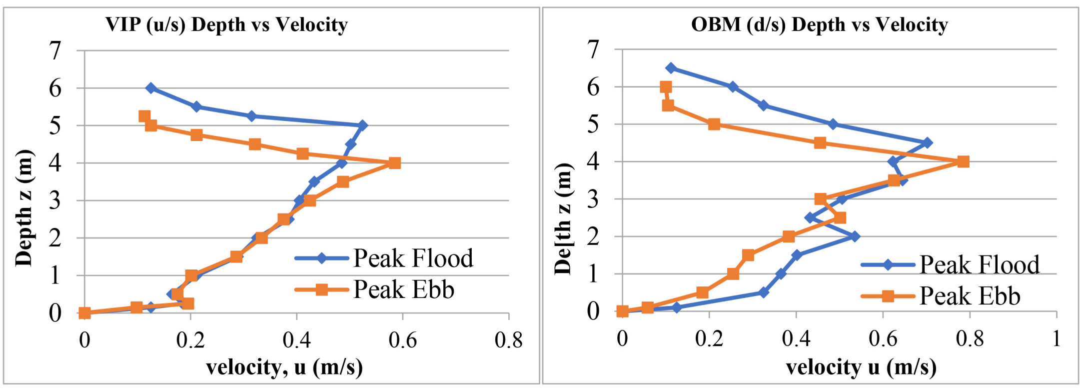

Figure S.1. Vertical velocity profile. Upstream location (left), downstream location (right).

Table S.1. Sediment concentration at VIP Ghat.

Depth (ft)	Half Tide	Full Tide	Half Ebb	Full Ebb
19		152.2		
18		154.5	32.2	
17.5	35.1			
16				45.8
15.5	40.2	161	35	
12.5	48	190.2	50	46.4
9.5	67.5	218.9	70.5	45
6.5	86	256.1	77.9	51.5
3.5	109	288.6	106.1	73
0.5	270	560	430	156.2
bottom				

Table S.2. Sediment concentration at OBM Ghat.

Depth (ft)	Half Tide	Full Tide	Half Ebb	Full Ebb
21	-	51.3	-	-
20	32.7		-	-
19			36.6	-
18.5	34	50		
18				35.5
15.5	33	57	39.3	36
12.5	38	64.5	47	46
9.5	52	81.9	61.5	38.3
6.5	118.8	130.5	72.7	50.1
3.5	128.8	157.5	110.4	95.5
0.5 (bottom)	670	690	560	406.7

Table S.3. Grain size limit classifications (ASTM D 7928-17), OBM Ghat and VIP Ghat.

	Gravel (>4.75 mm)	Sand (4.75 - 0.075 mm) 69.0%			Silt (0.075 - 0.005 mm)	Clay (0.005 - 0.001 mm)
		Coarse sand (4.75 - 2.00 mm)	Medium sand (2.00 - 0.425 mm)	Fine sand (0.425 - 0.075 mm)		
OBM Ghat	0.0%	0.0%	2.0%	67.0%	22.0%	8.0%
VIP Ghat	1.7%	0.0%	1.3%	70%	25%	1.0%

Table S.4. Grain size parameters (mm).

	D_{95}	D_{84}	D_{60}	D_{50}	D_{30}	D_{16}	D_{10}	D	$\sigma_1 = \frac{D_{84}-D_{16}}{4} + \frac{D_{95}-D_5}{6.6}$
OBM Ghat	0.3000	0.1800	0.1234	0.1042	0.0767	0.0300	0.0062	0.1047	0.082
VIP Ghat	0.3000	0.2000	0.1208	0.1049	0.0790	0.0400	0.0214	0.1049	0.073

Sediments become cohesive when the clay and silt contents are over 3% - 5% (Van Ledden, Van Kesteren, & Winterwerp, 2004). Here the clay particles are found 8%. Again, the sample may be termed as weakly cohesive if it contains 60% - 80% of sand (>62 μm) (van Rijn et al., 2007). Moreover, sediment will behave as cohesive when mud fraction (<0.05 mm) are 30% (van Rijn, 2012). Result shows that particle size < 0.05 mm for both locations are below 30%. Therefore, the sediment of the study site is weakly cohesive. Sorting of both samples are less than 0.350 indicating very well sorted and have undergone much transport (Folk, 1974).

Flow induced shear stress (τ_b) and shear velocity (u_*)

The current related bed shear velocity (u_*) and bed shear stress (τ_b) can be obtained from following equations:

$$u(z) = \frac{u_*}{k}\ln\left(\frac{z}{z_0}\right) \quad (A.1)$$

$$\text{and} \quad \tau_b = \rho_w u_*^2 \quad (A.2)$$

where z = vertical coordinate representing water depth, k = Von Karman's constant, usually taken as 0.4, and z_0 = vertical level with zero velocity, also often referred to as bed roughness. For hydraulically rough flow $z_0 = 0.033k_s$ where, k_s is bed roughness (Soulsby, 1997). During field measurement velocity was observed zero nearly at 0.1 m depth. Therefore, z_0 is reasonably taken as 0.1 m.

For OBM Ghat: for ebb condition u at z = 4 m is 0.785 m/s, z_0 = 0.1 m. Thus using Equations (A.1) & (A.2), $u_* = 0.085\ \text{m/s}$. [$0.785 = \frac{u_*}{0.4}\ln\left(\frac{4}{0.1}\right)$] and corresponding $\tau_b = 1023 \times (0.078)^2 = 7.41\ \text{N}\cdot\text{m}^{-2}$.

Similarly for flood condition u at z = 4.5 m is 0.702 m/s. Thus $u_* = 0.074\ \text{m/s}$ and $\tau_b = 5.57\ \text{N}\cdot\text{m}^{-2}$.

VIP Ghat: for ebb condition u at z = 4 m is 0.585 m/s, z_0 = 0.1 m. Thus $u_* = 0.063\ \text{m/s}$. $\tau_b = 1023 \times (0.063)^2 = 4.12\ \text{N}\cdot\text{m}^{-2}$.

For flood condition u at z = 5 m is 0.524 m/s. Thus $u_* = 0.054\ \text{m/s}$. and $\tau_b = 1023 \times (0.054)^2 = 2.94\ \text{N}\cdot\text{m}^{-2}$.

Critical shear velocity ($u_{*,cr,sus}$) and shear stress ($\tau_{*,cr,suspension}$) for suspension

For 20˚C and for $s = 2.61$, $\nu = 1.0 \times 10^{-6}\ \text{m}^2\cdot\text{s}^{-1}$. ν is kinematic viscosity that varies with temperature $= \frac{1.79 \times 10^{-6}}{1 + 0.03369T + 0.00021T^2}$ with temperature T in ˚C. Data was collected during winter season during day time in Bangladesh. The average water temperature was considered as 15˚C. For this temperature, $\nu = 1.15 \times 10^{-6}\ \text{m}^2\cdot\text{s}^{-1}$.

Here, $s = \rho_s/\rho_w = 2.6$ which is determined from laboratory test of bed material ($\rho_s = 2650\ \text{kg/m}^3$, $\rho_w = 1023\ \text{kg/m}^3$).

Thus for OBM Ghat, $D_* = \left[\frac{(s-1)g}{\upsilon^2}\right]^{1/3} D_{50} = 2.38$, when $D_{50} = 0.1042\ \text{mm}$ and for VIP Ghat $D_* = \left[\frac{(s-1)g}{\upsilon^2}\right]^{1/3} D_{50} = 2.39$, when $D_{50} = 0.1049\ \text{mm}$.

Critical Shield parameter for suspension obtained using Equation (1) is $\theta_{cr,suspension} = 0.099$.

Then the critical velocity component Equation (2), $u_{*,cr,suspension} = 0.0128\ \text{m/s}$. and $\tau_{*,cr,suspension} = \rho_w \times u^2_{*,cr,suspension} = 1023 \times 1.56 \times 10^{-4} = 0.167\ \text{N}\cdot\text{m}^{-2}$

Particle fall velocity w_s

Particle fall velocity for marine environment is estimated using Equation (3) as follows:

$$w_s = \frac{1.07 \times 10^{-6}}{1.042 \times 10^{-4}}\left[\left(10.36^2 + 1.049 \times 2.38^3\right)^{\frac{1}{2}} - 10.36\right] = 0.0073\ \text{m/s}$$

From grain size analysis, $D_{50} = 0.1042\text{ mm}$ and

$$D = \frac{D_{84} + D_{50} + D_{16}}{3} = 0.1047\text{ mm}.$$

Rouse Number, *N*

OBM Ghat: peak flood $N = \frac{w_s}{\beta\kappa u_*} = \frac{0.0073}{1\times 0.4\times 0.074} = 0.247$ and peak ebb $N = \frac{0.0073}{1\times 0.4\times 0.085} = 0.215$.

VIP Ghat: peak flood $N = \frac{w_s}{\beta\kappa u_*} = \frac{0.0073}{1\times 0.4\times 0.054} = 0.34$ and peak ebb $N = \frac{0.0073}{1\times 0.4\times 0.063} = 0.29$.

Estimated reference concentration, C_a and Transport Parameter *T*

OBM Ghat $T(\text{Peak ebb}) = \frac{\tau_b - \tau_{cr}}{\tau_{cr}} = \frac{u_*^2 - u_{*,cr}^2}{u_{*,cr}^2} = \frac{0.085^2 - 0.0128^2}{0.0128^2} = 43$ and $T(\text{Peak flood}) = \frac{0.074^2 - 0.0128^2}{0.0128^2} = 32.4$.

VIP Ghat $T(\text{Peak ebb}) = \frac{u_*^2 - u_{*,cr}^2}{u_{*,cr}^2} = \frac{0.063^2 - 0.0128^2}{0.0128^2} = 23$ and $T(\text{Peak flood}) = \frac{0.054^2 - 0.0128^2}{0.0128^2} = 16.8$.

At OBM Ghat when $T = 43$,

$$C_a = 0.015\frac{D_{50}T^{1.5}}{aD_*^{0.3}} = 0.015\frac{0.0001042\times 43^{1.5}}{0.16\times 2.39^{0.3}}.$$

$$= 2.12\times 10^{-3}\times 2650 = 5.62\text{ kg/m}^3 = 5620\text{ mg/L}$$

At VIP Ghat when $T = 23$, $C_a = 2198\text{ mg/L}$ and when $T = 16$, $C_a = 1275\text{ mg/L}$.

Evidence of rough bed condition

Analysis of measured data of the study site reveals that the current related bed shear velocity (0.074 - 0.085 m/s) is larger by 10% - 20% than critical velocity (0.0096 m/s). The median particle size of the bed material is 0.105 mm which is smaller than 0.5 mm. Water depth at the study site varies from 3 - 10 m which is >0.02 m. Transport stage parameter $T = 23 > 3$ and $D_* = 2.39$ which falls between 1 to 10. All these imply the presence of rough bed mostly with ripple formation. Flow depth where the velocity and sediment measurement were taken varies from 5 - 6 m. Therefore, for this study reference concentration $C(a)$ is taken at average of $0.05h$ and $0.01h$ between 0.15 - 0.165 m.